On the frequency response variation of sound field synthesis using linear arrays

Frank Schultz and Sascha Spors

Institute of Communications Engineering, University of Rostock, R.-Wagner-Str. 31 (Haus 8), D-18119 Rostock, Germany

E-Mail: {frank.schultz,sascha.spors}@uni-rostock.de

Introduction

Analytical driving functions for 2.5D sound field synthesis (SFS) with linear arrays using the single layer potential are typically derived for an infinite, continuous secondary source distribution (SSD) [1]. In practice spatially truncated and discretized SSDs are employed. This limits the spatial region and temporal frequency bandwidth for which the desired sound field is correctly synthesized. The paper considers a special case of SFS in synthesizing a cylindrical wave front perpendicular to the SSD (using the conventions and $k_x = 0$ rad/m of [1]). This corresponds to a pre-filtered infinite, continuous SSD with constant volume acceleration (i.e. minimum-phase 3dB/oct. lowpass characteristics, 3dB amplitude loss per distance doubling [2]) in order to obtain a flat frequency response at a reference line parallel to the SSD. A finite SSD exhibits spatial regions with more complex radiation characteristics. For ease of discussion, varying distances on the y-axis of a rect-windowed SSD are considered. The intended wave has frequency independent amplitudes and spherical monopole-like amplitude loss for low frequencies and/or far distances in the so-called Fraunhofer region. The so-called Fresnel region is valid for high frequencies and/or near distances and corresponds to the characteristics of the infinite SSD with constant volume acceleration, cf. fig. 1. Therefore SFS can only be approached within the Fresnel region of the SSD. The transition distance y_B between the Fresnel and Fraunhofer region is dependent on the SSD length L and frequency f. With speed of sound c it can be given as [3, I.3.d]

$$y_\mathrm{B}(f, L) = \frac{1}{2}\, L^2\, \frac{f}{c} \sqrt{1 - \frac{1}{(\frac{f}{c}\, L)^2}}, \qquad (1)$$

and graphically evaluated in fig. 2. Fig. 3 depicts sound pressure spectra on the main axis for a 4m rect-windowed SSD. For high frequencies ripples are observed due to the windowing, which can be analytically described by Fresnel integrals [3, I.3.b]. However at high frequencies the

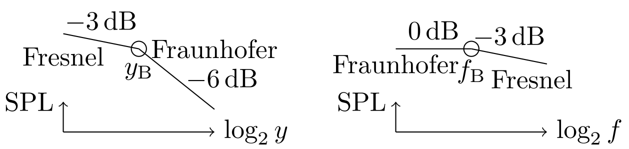

Figure 1: Simplified radiation characteristics for a rect-windowed SSD with constant volume acceleration on y-axis, cf. [2, 3]

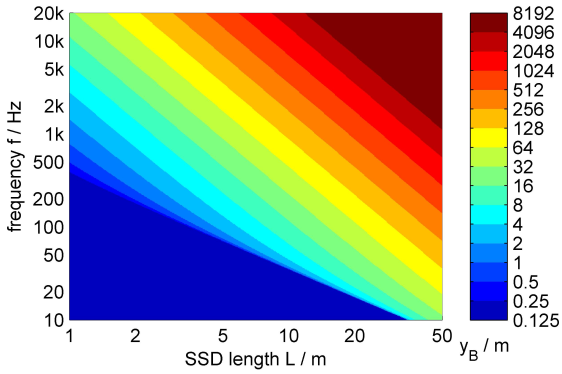

Figure 2: Transition distance y_B between Fresnel and Fraunhofer region on y-axis of a rect-windowed SSD with length L for cylindrical wave radiation perpendicular to the SSD. Air absorption is not considered.

amplitude loss of 3dB per distance doubling is preserved as intended for a cylindrical wave (Fresnel region). At low frequencies and far distances the amplitude loss is 6dB, rather than 3dB, which corresponds to the Fraunhofer region. The ideal prefilter [1, (17)] does not compensate the highpass-like slope. Therefore an adapted prefilter is required to obtain a flat frequency response at the reference line (x, y_ref) or rather the reference point $(0, y_\mathrm{ref})$, cf. [4].

Evaluation

In order to evaluate the interaction between different windows and a constant spatial SSD-discretization, the synthesized sound field was numerically calculated for positions $x/m = 0 : 0.25 : 1$, $y/m = 0.25 : 0.25 : 4$, $z/m = 0$

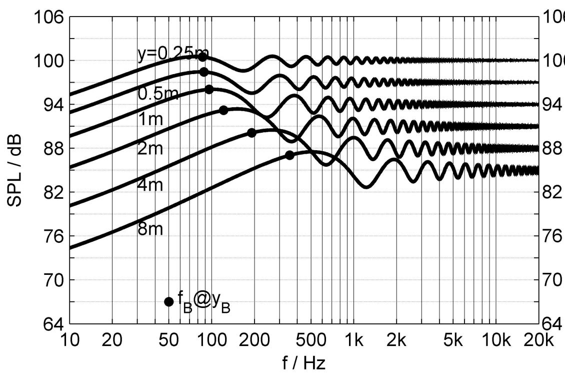

Figure 3: $|P(0, y, 0, \omega)|$ in $\mathrm{dB_{SPL}}$ of a rect-windowed, continuous, linear SSD with SDM-driving function [1, (17)], $k_x = 0$ rad/m, $y_\mathrm{ref} = 1$ m, $L = 4$ m, $c = 343$ m/s.

using [1, (9)]. For fig. 4-7 the following parameters were chosen: SDM-driving function [1, (17)], $k_x = 0\,\mathrm{rad/m}$, $y_{\mathrm{ref}} = 1\,\mathrm{m}$, SSD length $L = 4\,\mathrm{m}$, $c = 343\,\mathrm{m/s}$, SSD discretization $\Delta x = 0.2\,\mathrm{m}$. The ordinate indicates the evaluated x-values. For each x different y-values correspond to a 'slice' over frequency as indicated with the arrow in fig. 6. The plots are normalized to the sound pressure spectrum of $P(0, y_{\mathrm{ref}}, 0, \omega)$ to obtain a flat frequency response at this observation point (indicated as a black line corresponding to 0 dB deviation). In essence this compensates the highpass-like slope and the ripples which are due to the windowed SSD – observed in fig. 3 – with an adapted prefilter (cf. [4, fig. 1]). Note that this normalization method in the region of spatial aliasing frequencies should be avoided in practice. Furthermore the theoretical 3dB amplitude loss per distance doubling was compensated, thus the spectra show only the deviations from the ideal, expected behavior of a cylindrical wave. Levels > 1.5 dB and < -1.5 dB were clipped for a convenient observation of a frequency response deviation ± 1.5 dB. With [1, (38)] the theoretical spatial aliasing frequency for an infinite SSD is given as 1715 Hz.

The rect and Tukey windowed SSDs exhibit almost the same results with large frequency response variation due to the large ripples. The 'von Hann' windowed SSD produces the smoothest frequency responses, however within a smaller useable listening area $y_{\max} \approx 1.5$ m and $|x_{\max}| \approx 0.5$ m. With the Kaiser-Bessel window a trade-off between the frequency response variation and the useable listening area can be achieved via the parameter β (window main lobe width vs. side lobe attenuation). With $\beta = 2$ the area is extended to $y_{\max} \approx 2$ m, $|x_{\max}| = 0.75$ m with still acceptable level deviations over the whole audio bandwidth. Note the different characteristics of the spatial aliasing energy, which is due to the interaction of spatial truncation and discretization.

Conclusion

SFS should be used within the Fresnel region of a linear SSD. The effective listening area with small frequency deviations from the expected sound field characteristics strongly depends on the chosen SSD windowing and spatial discretization. For the presented example a Kaiser-Bessel window yields the largest area under accepting ± 1.5 dB level variation.

References

[1] Ahrens, J.; Spors, S. (2010): "Sound field reproduction using planar and linear arrays of loudspeakers." In: *IEEE Trans. Audio Speech Language Process.*, **18**(8):2038–2050.

[2] Lipshitz, S.P.; Vanderkooy, J. (1986): "The acoustic radiation of line sources of finite length." In: *Proc. of 81st Audio Eng. Soc. Convention, Los Angeles*, #2417.

[3] Heil, C.; Urban, M. (1992): "Sound fields radiated by multiple sound sources arrays." In: *Proc. of 92nd Audio Eng. Soc. Convention, Vienna*, #3269.

[4] Schultz, F.; Erbes, V.; Spors, S.; Weinzierl, S. (2013): "Derivation of IIR prefilters for soundfield synthesis using linear secondary source distributions." In: *Proc. of AIA-DAGA 2013, Merano, Italy*, 2372–2375.

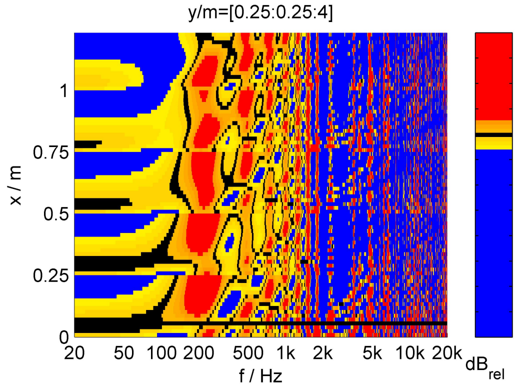

Figure 4: $|P(x, y, 0, \omega)|/|P(0, y_{\mathrm{ref}}, 0, \omega)|$ in dB, rect window.

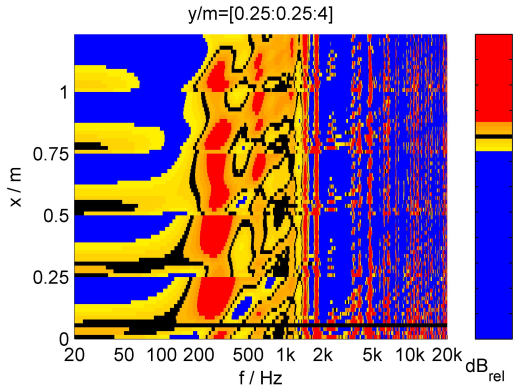

Figure 5: $|P(x, y, 0, \omega)|/|P(0, y_{\mathrm{ref}}, 0, \omega)|$ in dB, Tukey window (80% rect).

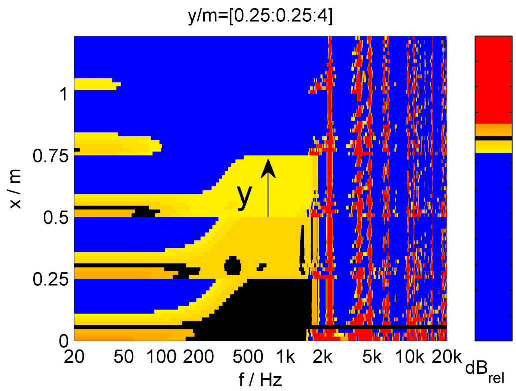

Figure 6: $|P(x, y, 0, \omega)|/|P(0, y_{\mathrm{ref}}, 0, \omega)|$ in dB, 'von Hann' window.

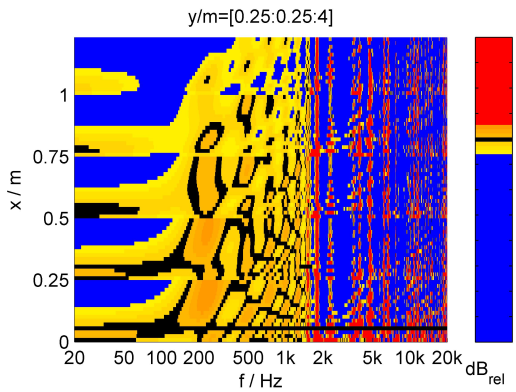

Figure 7: $|P(x, y, 0, \omega)|/|P(0, y_{\mathrm{ref}}, 0, \omega)|$ in dB, Kaiser-Bessel window $\beta = 2$.